ChemComm

Accepted Manuscript

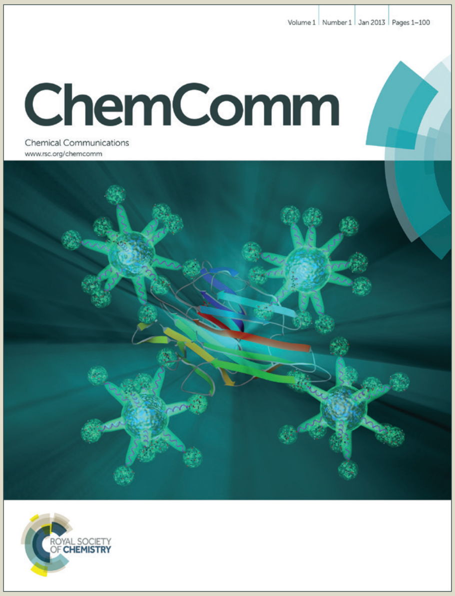

This is an *Accepted Manuscript*, which has been through the Royal Society of Chemistry peer review process and has been accepted for publication.

Accepted Manuscripts are published online shortly after acceptance, before technical editing, formatting and proof reading. Using this free service, authors can make their results available to the community, in citable form, before we publish the edited article. We will replace this *Accepted Manuscript* with the edited and formatted *Advance Article* as soon as it is available.

You can find more information about *Accepted Manuscripts* in the Information for Authors.

Please note that technical editing may introduce minor changes to the text and/or graphics, which may alter content. The journal's standard Terms & Conditions and the Ethical guidelines still apply. In no event shall the Royal Society of Chemistry be held responsible for any errors or omissions in this *Accepted Manuscript* or any consequences arising from the use of any information it contains.

ROYAL SOCIETY OF CHEMISTRY

www.rsc.org/chemcomm

ChemComm

COMMUNICATION

A New Approach for Bio-Jet Fuel Generation from Palm Oil and Limonene in absence of Hydrogen

Received 00th xx 20xx,
Accepted 00th xx 20xx

DOI: 10.1039/x0xx00000x

www.rsc.org/

Jingjing Zhang and Chen Zhao*

The traditional methodology includes carbon-chain shortening strategy to produce bio-jet fuel from lipids via a two-stage process with hydrogen. Here, we propose a new solution using a carbon-chain filling strategy to convert C_{10} terpene and lipids to jet fuel ranged hydrocarbons with aromatic hydrocarbons ingredients in absence of hydrogen.

Biologically derived jet fuel can be a key solution to the challenges faced by the aviation industry.[1-3] The traditional technique to produce bio-jet fuel from the lipid sources uses a “carbon-chain shortening strategy” (CSS) to reduce lipid carbon chain (ranging from C_{14} to C_{18}) to resemble that of kerosene (ranging from C_9 to C_{18}). This technique involves a two-step process. In the first step hydrodeoxygenation removes the oxygen atoms in the carbonyl groups to produce long-chain alkanes,[4-10] whereas the second step involves isomerization and non-selective C-C bond cracking steps to generate the range of paraffins which are suitable for jet fuel (C_9-C_{16} hydrocarbons) (Fig. 1a).[11-15]

The main problems faced by the CSS approach includes the consumption of large amounts of high pressurized H_2 during the two-stage process, substantial carbon loss in the cracking reaction, the need for the addition of extra aromatic hydrocarbons to the bio-jet fuel (around 25 vol%), and the necessity for running the two-stage process.[16] The consequences are therefore a low yield of kerosene ingredient (maximum yield: 50 wt%) and the high price of bio-jet fuel.[17] To overcome these disadvantages, we propose a novel solution which we refer to as “carbon-chain filling strategy” (CFS). The novelty of our approach relies on the new one-pot process based on co-activating lipid and monoterpene in the absence of external H_2 to produce bio-jet fuel ranged hydrocarbons with some fraction of aromatic hydrocarbons compositions.

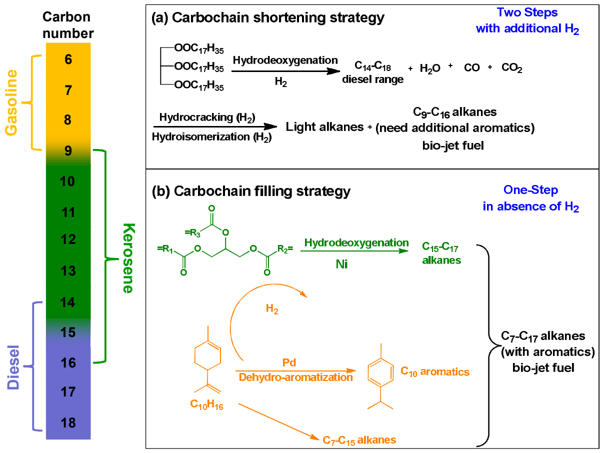

Figure 1. (a) Traditional carbon chain shortening strategy (CSS) for hydrodeoxygenation of triglyceride to bio-jet fuel via two steps in presence of H_2. (b) Proposed new carbon chain filling strategy (CFS) for hydrodeoxygenation of triglyceride to bio-jet fuel in a one-step process in the absence of H_2.

A C_{10} terpene was selected to co-activate lipid conversion in absence of external H_2, because the terpene releases both aromatic hydrocarbons and H_2,[18-19] and produces some smaller C_9-C_{15} alkanes. The formed aromatics and light alkanes can fill the gap for constructing a C_9-C_{16} kerosene-like jet fuel. The in-situ generated H_2 can be consumed by lipid to produce C_{14}-C_{18} alkanes via the hydrodeoxygenation route in a one-pot process. The exothermic hydrogenation and endothermic dehydrogenation steps are integrated into one process in order to maximize energy utilization (see Fig. 1b).

Limonene was used as a selected terpene for the dehydrogenation reaction carried out at relatively low temperatures of 200-300 °C, which was the similar range for lipid hydrodeoxygenation in the liquid phase.[20-22] However, this system is not free from challenges which include insufficient pressure of the generated hydrogen to hydrogenate the lipid, and incompatibility of the designed dual

---

Shanghai Key Laboratory of Green Chemistry and Chemical Processes, School of Chemistry and Molecular Engineering, East China Normal University, Shanghai 200062, China
E-mail: czhao@chem.ecnu.edu.cn

† Electronic Supplementary Information (ESI) available: Experimental details and data. See DOI: 10.1039/x0xx00000x

ChemComm Accepted Manuscript

active sites for dehydrogenation and hydrogenation. In addition, the side reactions of limonene condensation may prevent the target dehydrogenation step on limonene.

In the blank test with limonene in presence of N_2, limonene was very stable with a conversion lower than 4% at 280 °C. Subsequently, we selected a variety of Pd-based catalysts including Pd/C (activated carbon), Pd/ASA (amorphous silica alumina), Pd/SiO_2, Pd/Al_2O_3, Pd/Zeolite HBEA, Pd/Zeolite HY (SiO_2/Al_2O_3 ratio: 9-12), Pd/Zeolite HY (SiO_2/Al_2O_3 ratio: 30-60) and Pd/Zeolite HZSM-5 (SiO_2/Al_2O_3 ratio: 197) to catalyze limonene dehydroaromatization at 280 °C in the presence of N_2 (Fig. 2a, Electronic Supplementary Information Table S1). The results showed that Pd center seemed responsible for achieving a *p*-cymene yield of 60-80 wt.%, with dehydroaromatization rates of 616-634 $mmol \cdot g^{-1} \cdot h^{-1}$. Consistent with the kinetic curves of limonene conversion (Fig. S1), it was observed that limonene isomerization started as the first step, and the subsequent dehydrogenation reaction produced *p*-cymene and H_2. The in-situ release of H_2 from limonene over Pd/HZSM-5 achieved 18 bar pressure during the reaction with a dehydrogenation rate of 634 $mmol \cdot g^{-1} \cdot h^{-1}$. As the higher pressure would be more favorable for hydrogenation of the feedstock of stearic acid or other lipids, and thus, Pd/HZSM-5 was selected as the catalyst for further investigation.

The single Pd/HZSM-5 catalyst showed a poor performance towards stearic acid hydrodeoxygenation in limonene with a conversion rate of 14% at 280 °C with N_2, so the second metal was incorporated in order to improve the desired activity. The addition of Co, Cu, Fe, Zn, and Rh aided with the second Pd center by the co-impregnation method was shown to be inactive for stearic acid hydrodeoxygenation in limonene at identical conditions (Fig. 2b, Table S2). By adding the Ru site to Pd, the bimetallic RuPd/HZSM-5 catalyzed around 50% hydrocarbon yield (mainly C_{17} and C_{18}) from stearic acid in limonene at 280 °C with N_2. It was surprising that the addition of Ni sharply increased the C_{17}/C_{18} hydrocarbons to nearly 100% from stearic acid conversion while maintaining a 70% *p*-cymene yield from limonene conversion, making a good use from simultaneous dehydrogenation of limonene over Pd, H· transfer from Pd to Ni, and hydrodeoxygenation of stearic acid over Ni in a one-pot process.

In terms of the kinetics of the chemical conversion process, Fig. 2c and Fig. 2d present the respective kinetics curves of the two feedstock. Limonene followed initial isomerization and partial hydrogenation pathway and finally underwent dehydroaromatization to produce *p*-cymene, reaching an initial dehydrogenation rate of 204 $mmol \cdot g^{-1} \cdot h^{-1}$. On the other hand, firstly stearic acid was esterified with fatty alcohol (formed by hydrogenation of stearic acid) as a primary product with a rate of 5.3 $mmol \cdot g^{-1} \cdot h^{-1}$, then was subjected to the sequential C-O bond cleavage and finally the decarbonylation of the ester led to final long-chain alkanes formation (Table S3, Fig. S2). The durability of PdNi/HZSM-5 catalyst was evaluated by stearic acid conversion in limonene at 280 °C in the presence of N_2 at 0.8 MPa for 2 h. The obtained activity (100% conversion after 2 h) and selectivity (100% after 2 h) were consistent in the consecutive four recycling tests and demonstrated that the developed PdNi/HZSM-5 catalyst exhibited high stability in this catalytic system (Fig. S3).

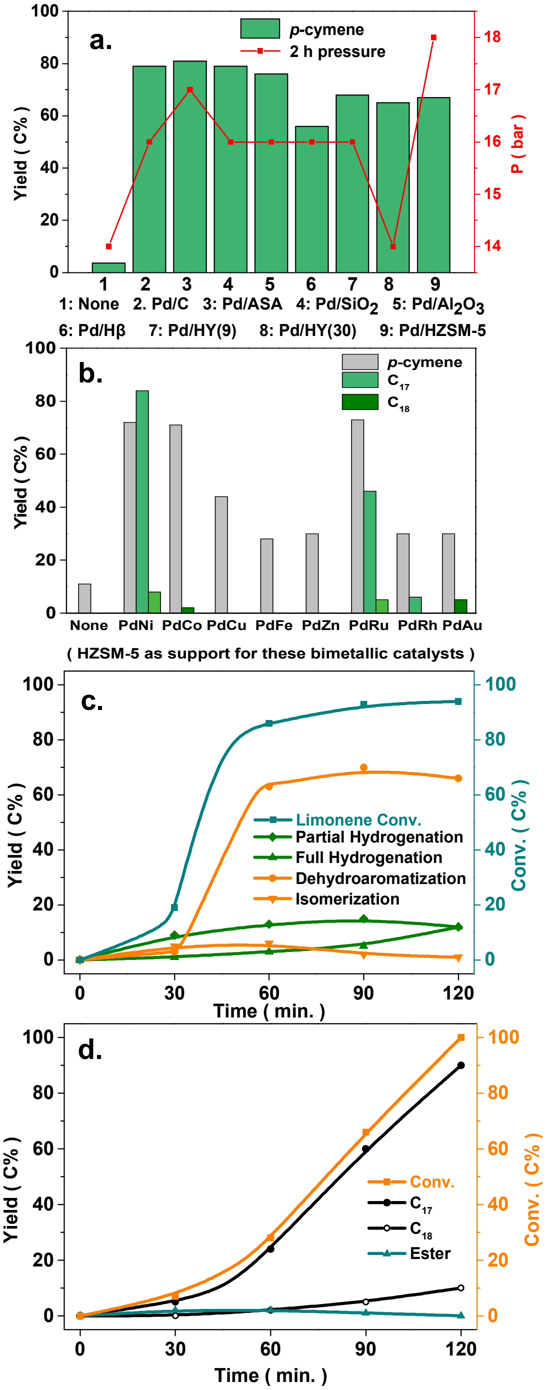

Figure 2. (a) Yields of dehydroaromatization of limonene with diverse supported 1% Pd catalysts. Conditions: 10 mL limonene, 80 mL *n*-dodecane, 2 h. (b) Product distributions for stearic acid hydrodeoxygenation in limonene with bimetallic Pd-M/HZSM-5 catalysts. Conditions: 1.0 g stearic acid, 50 mL limonene, 2 h. Product distributions for (c) limonene dehydroaromatization and (d) stearic acid hydrodeoxygenation in the overall reaction with PdNi/HZSM-5 as a function of time. Conditions: 1.0 g stearic acid, 50 mL limonene. General conditions: 0.20 g catalysts, 280 °C, 0.8 MPa N_2, stirring at 650 rpm.

ChemComm Accepted Manuscript

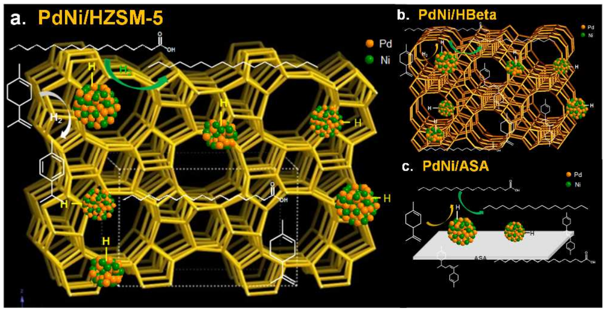

Figure 3. The influence of pore structures of (a) PdNi/HZSM-5, (b) PdNi/HBEA, (c) PdNi/ASA for changing products from co-activation of limonene and stearic acid in a one-pot process in absence of H_2.

Another interesting observation was that the pore properties of the supports greatly influenced the product distributions. Three typical acidic supports of zeolite HZSM-5, zeolite HBEA, and amorphous silica alumina (ASA) were chosen to construct respective PdNi based catalysts. The latter two samples poorly catalyzed stearic acid conversions at low alkane yields (1% and 0%, respectively) in limonene (Fig. 3, Fig. S4), and also they highly promoted side-reactions of limonene condensations. Brönsted acid sites (BAS) of HZSM-5 and HBEA were located in the 10-ring and 12-ring pores, while BAS of the ASA support was situated on the external surface of open pores. The calculated diameter for the limonene condensation product was around 5.8 Å (see Fig. S5), while the pore sizes of HBEA and HZSM-5 are 6.6-7.7 Å and 5.1-5.6 Å, respectively. Therefore, the unconfined pores in ASA and large pores in HBEA both help to form limonene condensation products, whereas the proper pore size and the suitable acidity of HZSM-5 ensure the occurrence of the targeted coupled reactions of limonene dehydroaromatization and stearic acid hydrodeoxygenation within an integrated process.

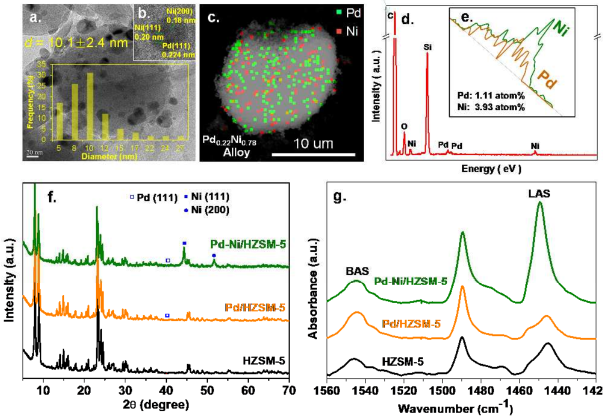

Figure 4. Characterization of the used PdNi/HZSM-5 catalyst by (a) TEM and (b) HRTEM images, (c) SEM-mapping image, (d) SEM-EDX, (e) STEM-EDX analysis of bimetallic PdNi nanoparticles. (f) XRD patterns and (g) IR spectra of adsorbed pyridine towards three samples of HZSM-5, Pd/HZSM-5, and PdNi/HZSM-5.

We characterized the bimetallic PdNi/HZSM-5 catalyst (SiO_2/Al_2O_3 ratio of 197). The particle size of this catalyst prepared by co-impregnating method was 10.1 ± 2.4 nm, as determined from TEM image (Fig. 4a). High-resolution TEM image (Fig. 4b) showed the lattice fringes of fcc Ni (200), Ni (111) and Pd (111), indicating that PdNi nanoparticles were composed of single- crystallinity or twin-crystallinity particles. The SEM-mapping and STEM-EDX spectra of PdNi/HZSM-5 both demonstrated that the bimetallic dispersive Ni and Pd nanoparticles were embedded in an alloy-like structure (Fig. 4c). The SEM-EDX analysis indicated that the surface of such catalyst contained 1.11 atom% Pd and 3.93 atom% Ni (Figs. 4d-4e), confirming that the formed bimetallic PdNi nanoparticles ($Pd_{0.20}Ni_{0.80}$) basically agreed with the nominal composition ($Pd_{0.22}Ni_{0.78}$). The XRD patterns (Fig. 4f) indicated a mixture of fcc Ni (200), fcc Ni (111), and fcc Pd (111) phase was in the form of PdNi nanoparticles, consistent with the information from HRTEM results. The acid sites as probed by IR spectra of adsorbed pyridine (Fig. 4g) showed that PdNi/HZSM-5 had 92 mmol·g^{-1} Brönsted acid site and 208 mmol·g^{-1} Lewis acid site (Table S4).

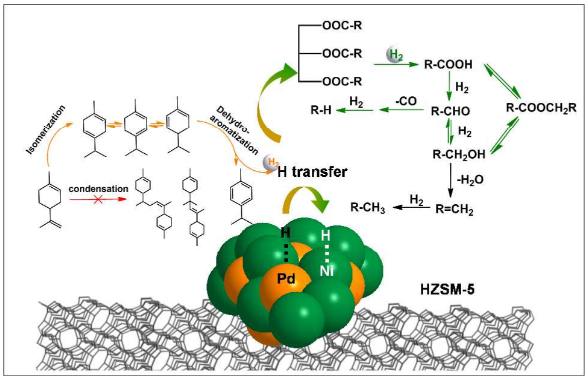

Figure 5. Proposed mechanism for co-activation of palm oil and limonene on the surface of PdNi/HZSM-5 with internal hydrogen transfer.

The data suggest that the dispersed Pd and Ni nanoparticles loaded on the PdNi/HZSM-5 catalyst may play a beneficial role for in-situ produced H· transfer on the surface of PdNi alloy, and the proper pore size of HZSM-5 support (5.1-5.6 Å) prevents the side-reaction (limonene condensation product, diameter: 5.8 Å) from occurring (Fig. 5).

Finally, we used this optimized technique for co-activation of palm oil and limonene in the presence of the PdNi/HZSM-5 catalyst at 280 °C in the absence of H_2. The fatty acid composition of the used palm oil was analyzed by the transesterification method with methanol, and mainly composed of saturated C_{16} fatty acids (36%), and C_{18} fatty acids (including 12% saturated and 50% unsaturated components) (Table S5). The catalysis test quantitatively showed that palm oil and limonene were converted to a hydrocarbon mixture ranging from 4 to 18 carbons (including a large fraction of aromatic hydrocarbons, Fig. S7) after 2 h using the optimized catalysis system (Fig. 6a, Table S6). Such formed hydrocarbon mixture was analogical to the compositions and properties of commercial bio-jet fuel, please refer to GC-MS analysis of kerosene purchased from SINOPEC as displayed in Fig. S8. A trace amount of toluene (1.2%) was observed, as formed by eliminating 1 mole of C_3H_8 from *p*-cymene. In addition, a yield of 3% limonene condensation products was also produced.

ChemComm Accepted Manuscript

The major gas-phase component (Fig. 6b) was H_2 derived from limonene dehydrogenation. In addition, trace amounts of CO and CO_2 (formed in decarbonylation and decarboxylation reactions), CH_4 (generated by methanation of CO and CO_2 with H_2), C_3H_8 (released by C-C cracking of *p*-cymene), and other lighter alkanes (C_2H_6, C_2H_4, *i*-, *n*- C_4H_{10}, and *i*-, *n*- C_5H_{12}) were also detected (Table S6).

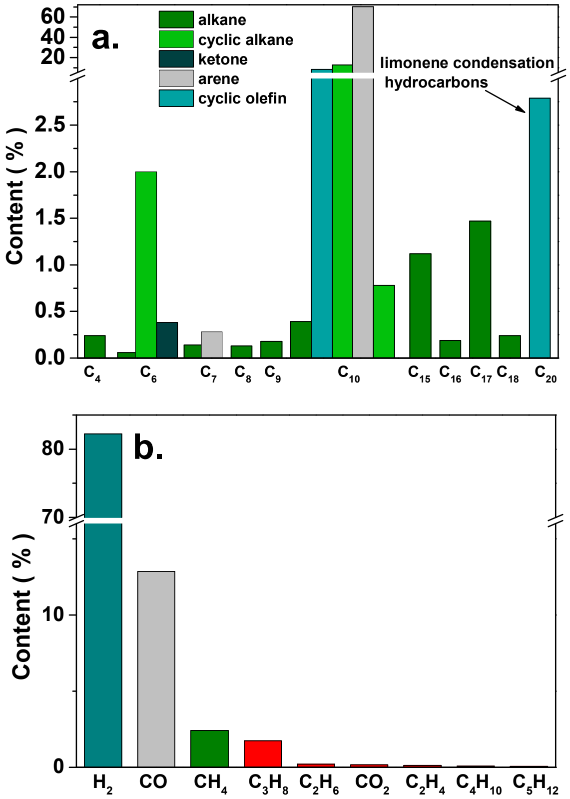

Figure 6. (a) Liquid phase and (b) gas phase products for co-reaction of palm oil and limonene in the absence of H_2.

In co-activation of palm oil and limonene over PdNi/HZSM-5 in the absence of H_2, the hydrocarbon products (C_{15}, C_{16}, C_{17} and C_{18}) linearly increased from palm oil conversion as a function of time reaching a rate of 2.35 $g_{oil}\cdot g^{-1}\cdot h^{-1}$. At the same time, the H_2 donor - limonene underwent sequential isomerization and dehydrogenation to produce H_2 and *p*-cymene at a rate of 492 $mmol\cdot g^{-1}\cdot h^{-1}$ (Figs. S9a and S9b). The in-situ H_2 was a direct reactant for palm oil hydrodeoxygenation which also promoted the equilibrium shift for the hydrogenation-dehydrogenation reaction of limonene.

In summary, we demonstrate a novel approach for the conversion of palm oil and limonene to bio-jet fuel ranged hydrocarbons without the need of hydrogen. Using a PdNi/HZSM-5 zeolite catalyst, a monoterpene can release aromatic hydrocarbons and hydrogen and smaller C_9-C_{15} alkanes at 280 °C. The in-situ generated hydrogen from terpene dehydroaromatization enables the hydrodeoxygenation of lipid to C_{14}-C_{18} alkanes. We show that lighter alkanes and aromatic hydrocarbons are produced from limonene simultaneously with C_{14}-C_{18} hydrocarbons generated from lipids, filling the gap for essential ingredients for a perfect composition of bio-jet fuel.

The cascade reactions for palm oil and limonene co-activation at moderate temperature under the inert N_2 atmosphere lead to high yields of bio-jet fuel in a simple, efficient, and green way. By directly boiling the two biomass feedstock it is possible to solve the high-demand issues for H_2, aromatics and light alkanes for production of the bio-jet fuel in a highly integrated one-pot process. Future studies would focus on a more detailed characterization of the properties of resultant bio-jet fuel and experiments to optimize the process at an industrial scale.

We gratefully acknowledge the financial support from the Recruitment Program of Global Young Experts in China, National Natural Science Foundation of China (Grant No. 21573075), and Shanghai Pujiang Program (No. PJ1403500).

Notes and references

1 A. Corma, S. Iborra and A. Velty, *Chem. Rev.*, 2007, **107**, 2411.
2 G. W. Huber, S. Iborra and A. Corma, *Chem. Rev.*, 2006, **106**, 4044.
3 K. S. Arias, M. J. Climent, A. Corma and S. Iborra, *Energy Environ. Sci.*, 2015, **8**, 317.
4 E. L. Kunkes, D. A. Simonetti, R. M. West, J. C. Serrano-Ruiz, C. A. Gärtner and J. A. Dumesic, *Science*, 2008, **322**, 417.
5 D. M. Alonso, S. G. Wettstein and J. A. Dumesic, *Chem. Soc. Rev.*, 2012, **41**, 8075.
6 J. Q. Bond, A. A. Upadhye, H. Olcay, G. A. Tompsett, J. Jae, R. Xing, D. M. Alonso, D. Wang, T. Zhang, R. Kumar, et al., *Energy Environ. Sci.*, 2014, **7**, 1500.
7 D. Verma, R. Kumar, B. S. Rana and A. K. Sinha, *Energy Environ. Sci.*, 2011, **4**, 1667.
8 M. Snåre, I. Kubičková, P. Mäki-Arvela, K. Eränen and D. Y. Murzin, Ind. *Eng. Chem. Res.*, 2006, **45**, 5708.
9 B. Rozmysłowicz, P. Mäki-Arvela, A. Tokarev, A. Leino, K. Eränen and D. Y. Murzin, *Ind. Eng. Chem. Res.*, 2012, **51**, 8922.
10 G. J. S. Dawes, E. L. Scott, J. L. Nôtre, J. P. M. Sanders and J. H. Bitter, *Green Chem.*, 2015, **17**, 3231.
11 L. Petrus and M. A. Noordermeer, *Green Chem.*, 2006, **8**, 861.
12 A. Corma, V. González-Alfaro and A.V. Orchillés, *J. Catal.*, 2001, **200**, 34.
13 M. Snåre, I. Kubičková, P. Mäki-Arvela, K. Eränen and D. Y. Murzin, *Fuel*, 2008, **87**, 933.
14 J. G. Immer, M. J. Kelly and H. H. Lamb, *Appl. Catal. A*, 2010, **375**, 134.
15 S. P. R. Katikaneni, J. D. Adjaye and N. N. Bakhshi, *Energy & Fuels*, 1995, **9**, 1065.
16 C. Zhao, T. Brück and J. A. Lercher, *Green Chem.*, 2013, **15**, 1720.
17 C. O. Tuck, E. Pérez, I. T. Horváth, R. A. Sheldon and M. Poliakoff, *Science*, 2012, **337**, 695.
18 C. Zhao, W. Gan, X. Fan, Z. Cai, P. J. Dyson and Y. Kou, *J. Catal.*, 2008, **254**, 244.
19 Y. Gu and F. Jérôme, *Chem. Soc. Rev.*, 2013, **42**, 9550.
20 B. Ma and C. Zhao, *Green Chem.*, 2015, **17**, 1692.
21 B. Peng, Y. Yao, C. Zhao and J. A. Lercher, *Angew. Chem. Int. Ed.*, 2012, **51**, 2072.
22 B. Ma, J. Hu, Y. Wang and C. Zhao, *Green Chem.,* 2015, **17,** 4610.

ChemComm Accepted Manuscript

This journal is © The Royal Society of Chemistry 2015

Table of Content:

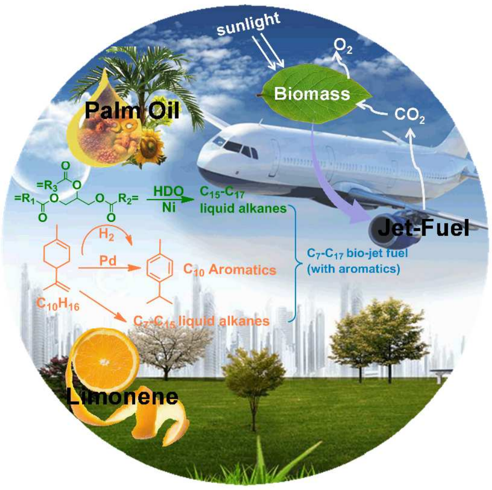

ChemComm Accepted Manuscript